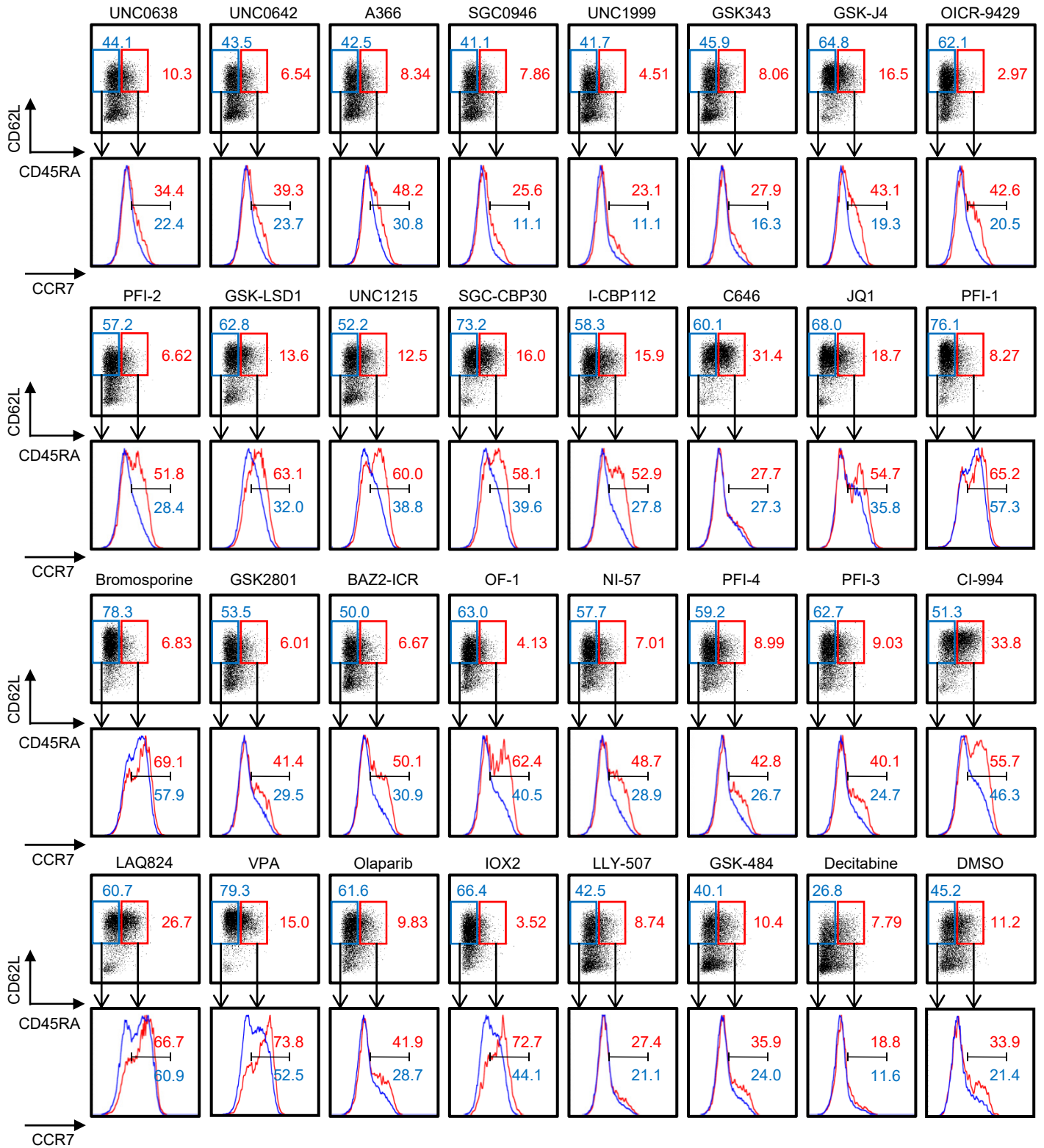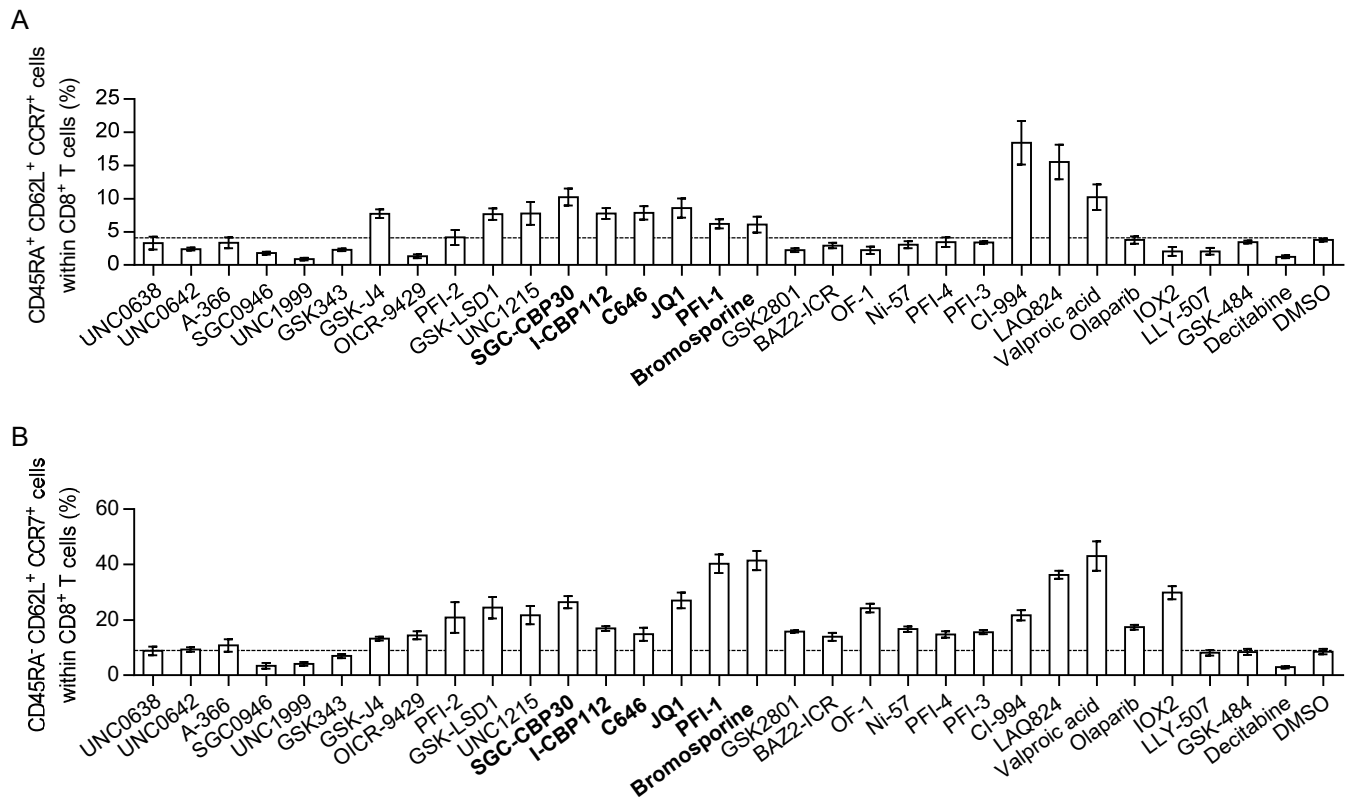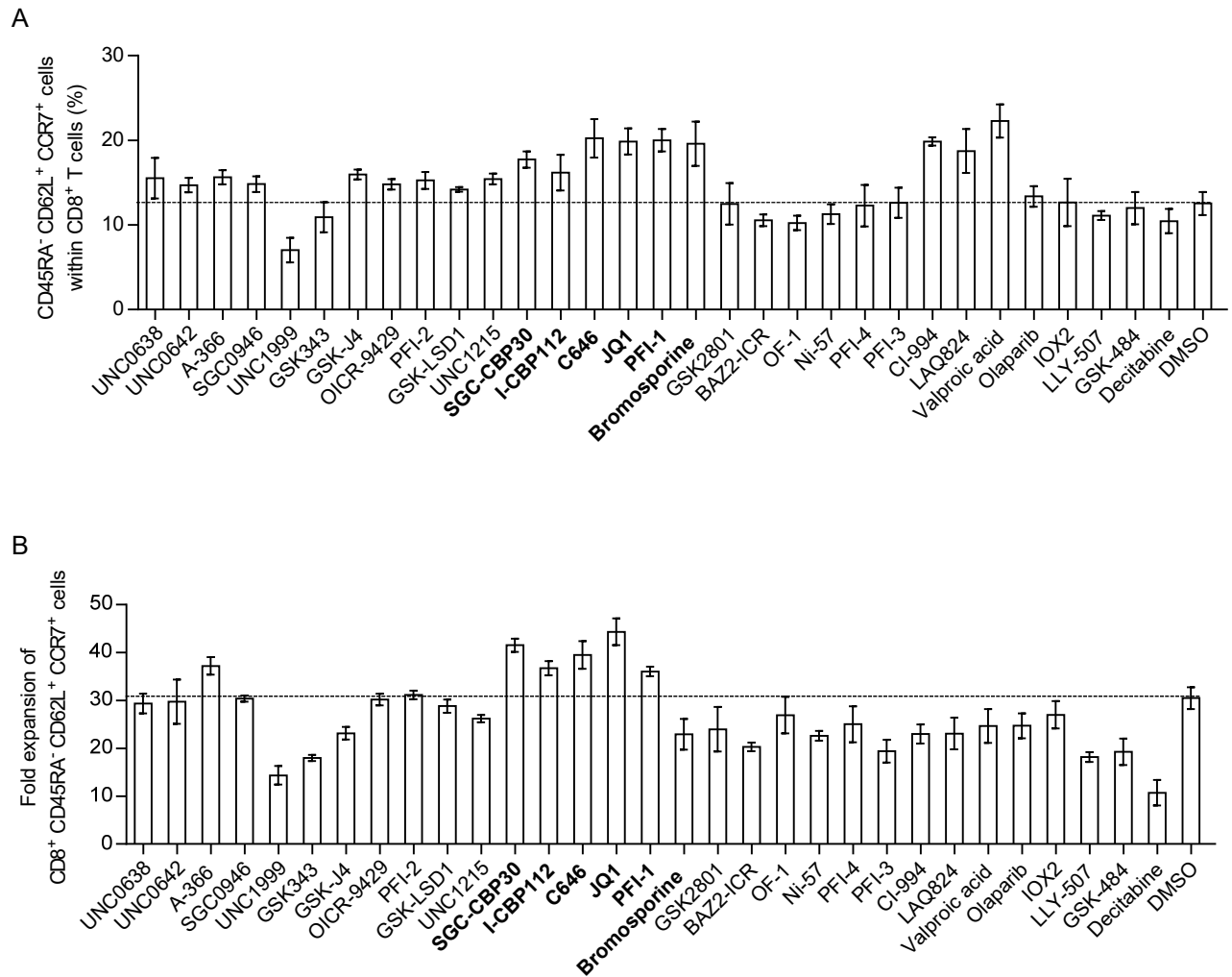# Supplemental Figure 1

Supplemental Figure 1. Screening of epigenetic targets that affect the differentiation status of CD8$^+$ T cells. Flow cytometry plots of CD45RA, CD62L and CCR7 expression in CD8$^+$ T cells treated with each chemical probe 14 days following initial stimulation with aAPC/mOKT3.

Supplemental Figure 2. Effects of epigenetic chemical probes on CD8$^+$ T cell differentiation. (A, B) Frequency of CD45RA$^+$ CD62L$^+$ CCR7$^+$ (A) and CD45RA$^-$ CD62L$^+$ CCR7$^+$ cells (B) within CD8$^+$ T cell population cultured for 14 days in the presence of each chemical probe. Inhibitors for p300 and BET proteins are indicated in bold. The error bars indicate the S. D. of three technical replicates. The dotted lines indicate the mean values in DMSO control wells.

A

B

Supplemental Figure 3. Effects of epigenetic targets on differentiation of CD45RO$^+$ memory T cells. (A, B) Peripheral blood CD3$^+$ CD45RO$^+$ T cells were stimulated with aAPC/mOKT3 and subsequently treated with each epigenetic chemical probe. The frequency (A) and absolute fold expansion (B) of CD45RA$^-$ CD62L$^+$ CCR7$^+$ cells within the CD8$^+$ T cell population 14 days following initial stimulation are shown. Inhibitors for p300 and BET proteins are indicated in bold. The error bars indicate the S. D. of three technical replicates. The dotted lines indicate the mean values in DMSO control wells.
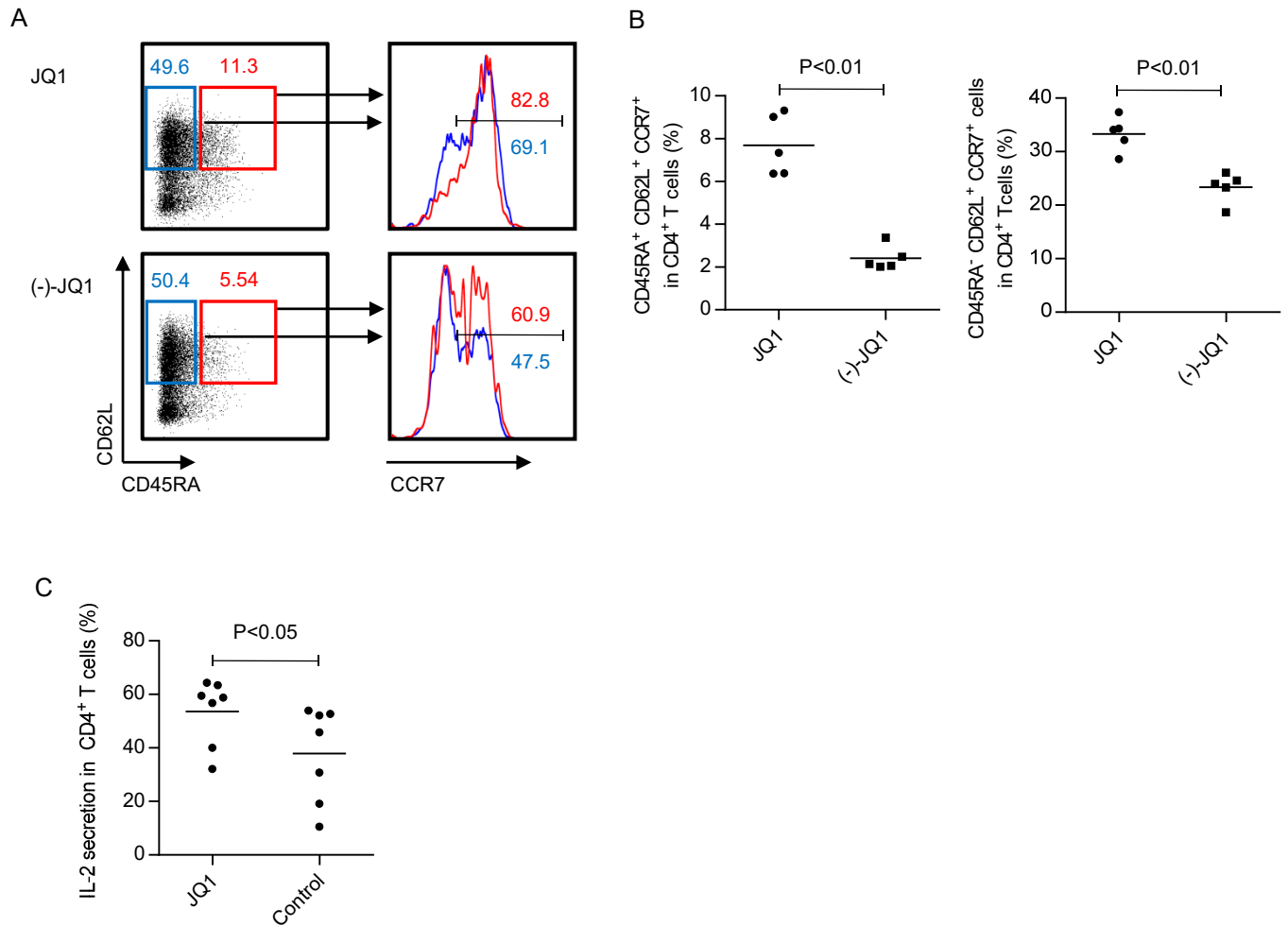
Supplemental Figure 4

A

B
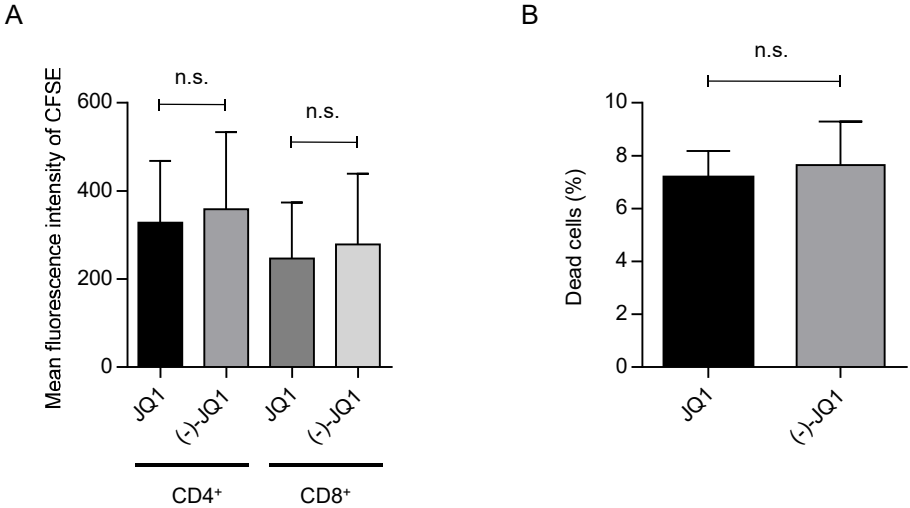
**Supplemental Figure 4. Effects of JQ1 treatment on T cell division rate and viability.** (A, B) CD3^{+} T cells labeled with CFSE were stimulated with aAPC/mOKT3 and cultured in the presence of JQ1 or (-)-JQ1 for 3 days. The average mean fluorescence intensity of CFSE in CD4^{+} and CD8^{+} T cells (A) as well as the frequency of dead cells (B) were evaluated by flow cytometry (n=5). Error bars depict the S. D.

Supplemental Figure 5

A

CD62L

CD45RA

CCR7

B

C

Supplemental Figure 5. Differentiation status of CD4$^+$ T cells treated with JQ1. (A, B) CD45RA$^+$ CD62L$^+$ CCR7$^+$ T cells were stimulated weekly with aAPC/mOKT3 and cultured in the presence or absence of JQ1. Representative FACS plots showing expression of CD45RA, CD62L and CCR7 (A), and the frequency of CD45RA$^+$ CD62L$^+$ CCR7$^+$ and CD45RA$^-$ CD62L$^+$ CCR7$^+$ cells within the CD4$^+$ T cell population 21 days following initial stimulation is shown (B; n=5, paired t test). (C) IL-2 secretion upon restimulation with aAPC/mOKT3 in CD4$^+$ T cells cultured for 14 days with or without JQ1 (n=7, paired t test).

Supplemental Figure 6
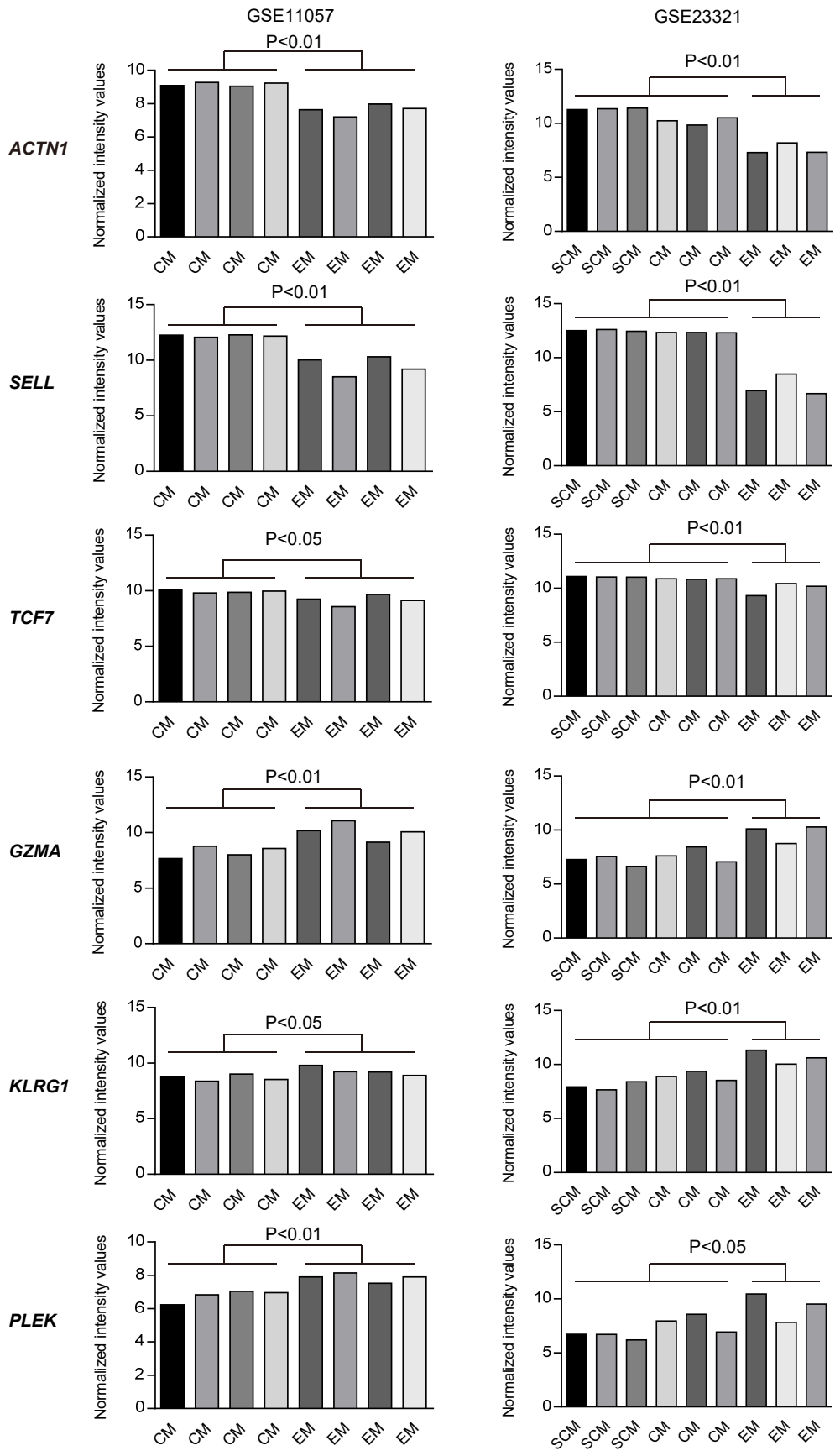
Supplemental Figure 6. Differentially expressed genes between the T_{SCM}/T_{CM} and T_{EM} phenotypes. Normalized intensity values of the indicated genes from the published microarray data (GSE11057 and GSE23321) are shown.

Supplemental Figure 7. Comparison of the functional properties of CD45RO$^+$ memory T cells treated with JQ1 or (-)-JQ1.
(A) CD3$^+$ CD45RO$^+$ cells were stimulated with aAPC/mOKT3 and cultured with JQ1 or (-)-JQ1 for 14 days. The frequency of CD45RA$^-$ CD62L$^+$ CCR7$^+$ cells within the CD8$^+$ T cell population is shown (n=8, paired t test). (B, C) CD45RO$^+$ T cells treated with JQ1 or (-)-JQ1 for 14 days were restimulated with aAPC/mOKT3, and the production of IL-2, IFN-γ and TNF-α in CD8$^+$ T cells was assessed with intracellular flow cytometry. The frequency of individual cytokine-secreting cells (B) and those producing all three cytokines (C) is shown (n=4, paired t test). (D) Expression profiles of representative genes with differential expression between the T$_{CM}$ and T$_{EM}$ phenotypes. The average expression levels in the JQ1-treated CD8$^+$ T cells relative to those in (-)-JQ1-treated CD8$^+$ T cells are shown (n=4). Error bars indicate the S. D.
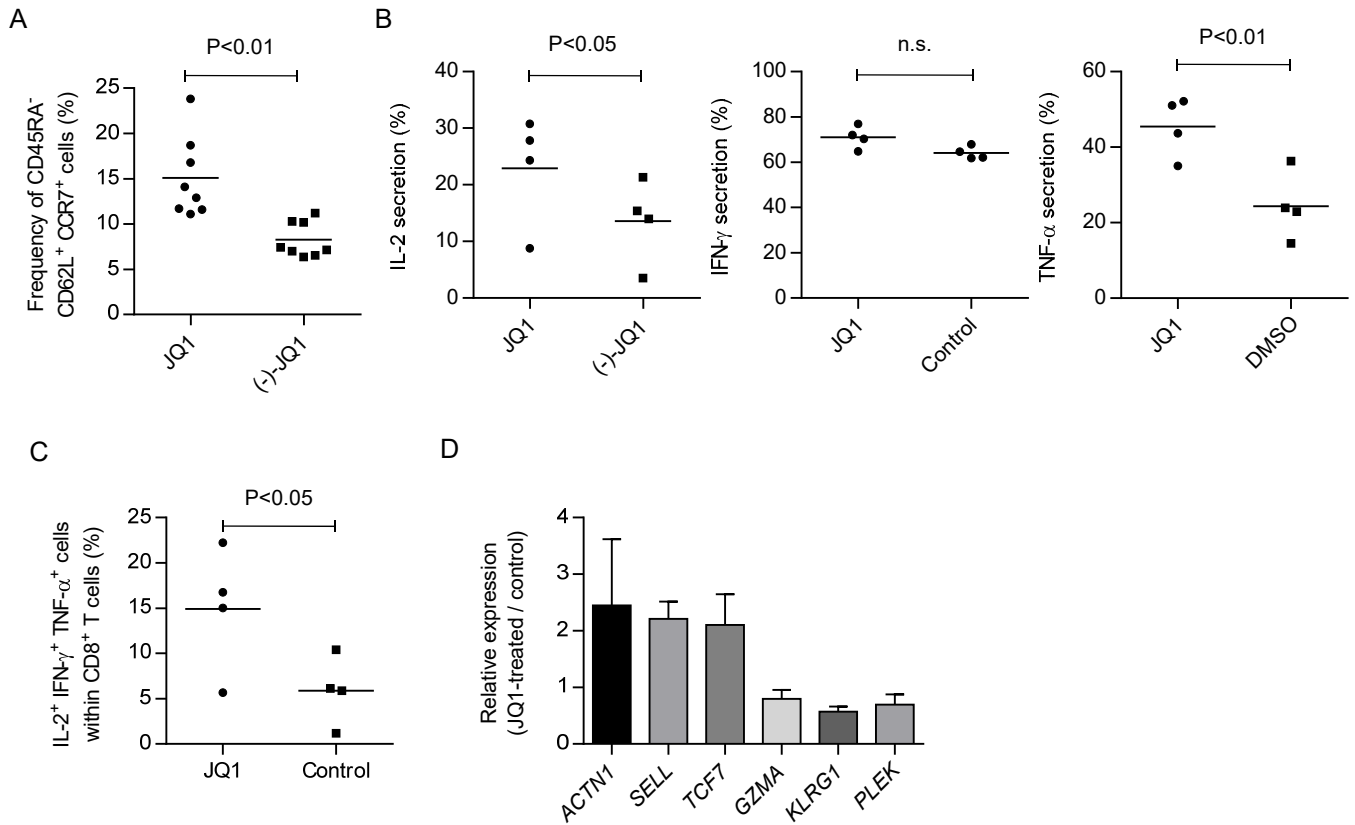
Supplemental Figure 8
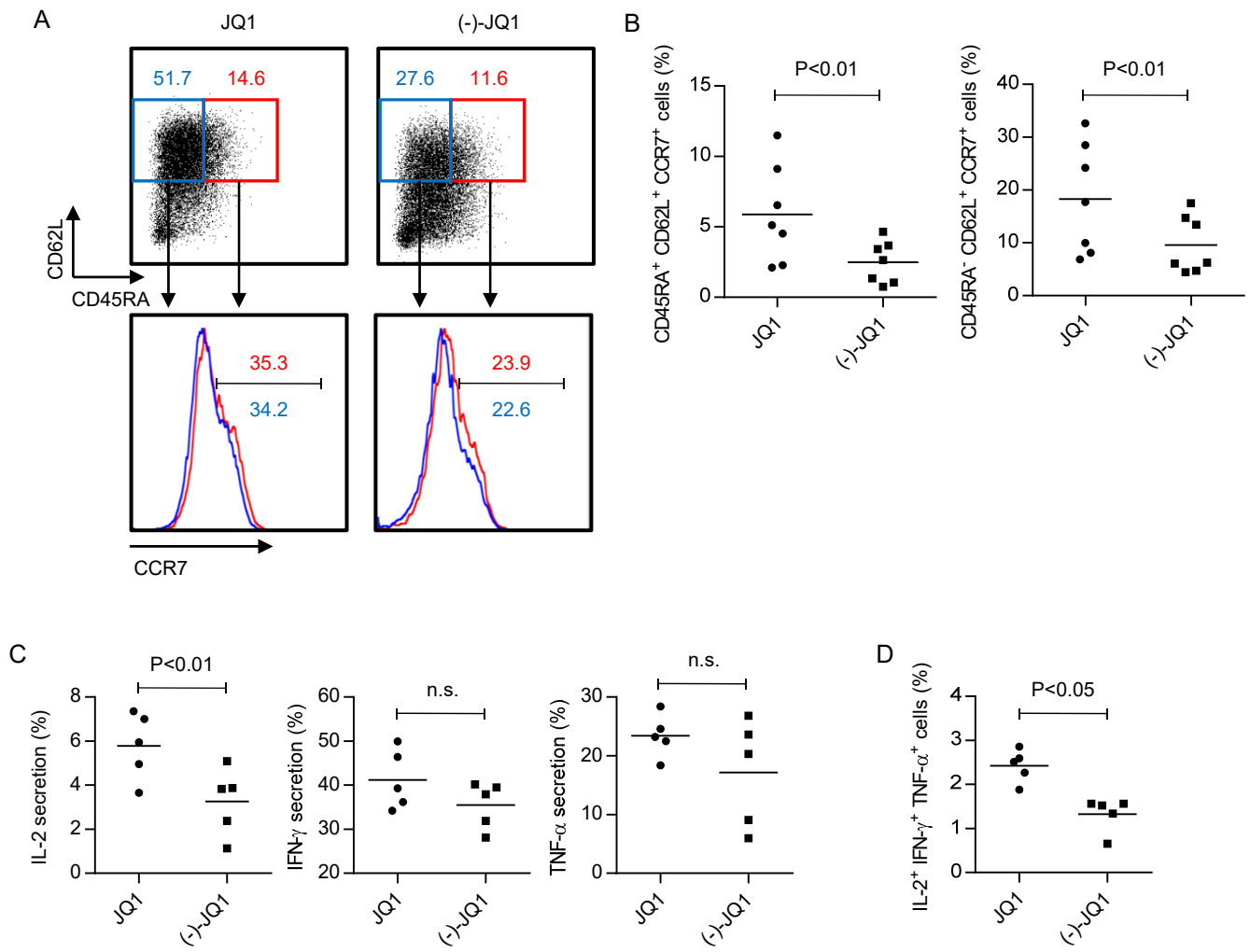
Supplemental Figure 8. Effects of JQ1 on CD8^{+} T cell differentiation in the absence of costimulatory signals. (A, B) CD3^{+} T cells were stimulated every week with plate-coated anti-CD3 mAb (clone OKT3) and cultured in the presence or absence of JQ1. Representative FACS plots (A) and the frequencies of CD45RA^{+} CD62L^{+} CCR7^{+} and CD45RA^{-} CD62L^{+} CCR7^{+} cells (B) within the CD8^{+} T cell population 14 days following the initial stimulation (n=7, paired t test). (C, D) Secretion levels of IL-2, IFN-γ, and TNF-α were evaluated by intracellular flow cytometry in JQ1- and (-)-JQ1-treated CD8^{+} T cells. The frequencies of each type of cytokine-secreting cells (C) and cells producing all three cytokines (D) are shown (n=5, paired t test).

Supplemental Figure 9
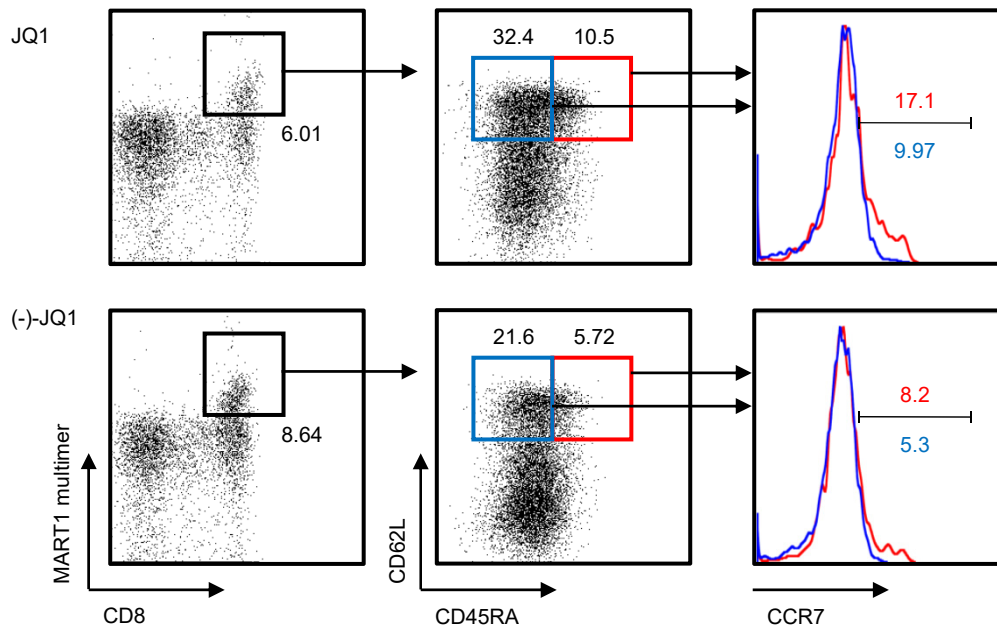
Supplemental Figure 9. Differentiation of CD8+ T cells upon antigen-specific T cell stimulation. CD3+ T cells were stimulated weekly with aAPC/A2 loaded with mutant MART1$_{27–35}$ peptide in the presence of JQ1 or (-)-JQ1. The CD8+ A2/MART1 multimer+ cells were analyzed for CD45RA, CD62L and CCR7 expression 21 days after initial stimulation. Representative FACS plots of four independent experiments are shown.

Supplemental Figure 10. Cytokine secretion by CAR-transduced T cells following restimulation with K562-CD19. JQ1- or (-)-JQ1-treated CAR-T cells were stimulated with K562-CD19 in the absence of drugs. Five days later, they were restimulated with K562-CD19, and cytokine secretion was evaluated by intracellular flow cytometry. Frequencies of each type of cytokine-producing cell and cells secreting all three cytokines are shown (n=5, paired t test).
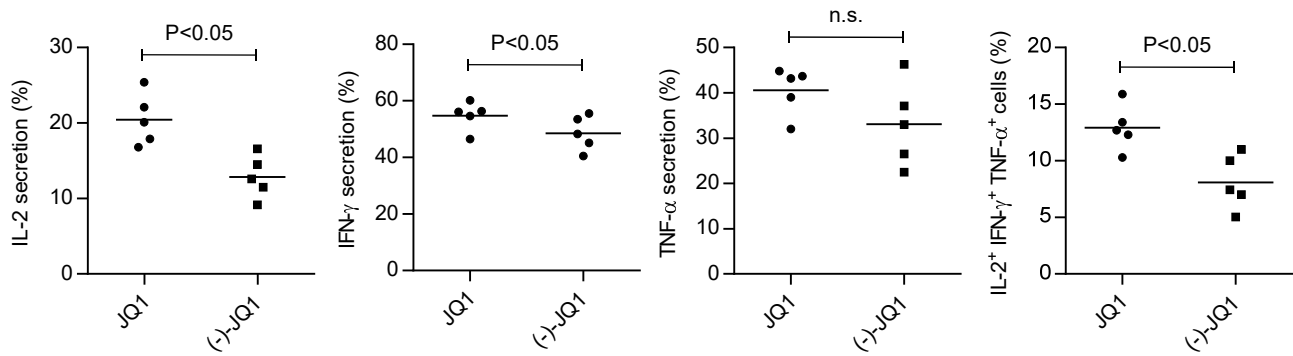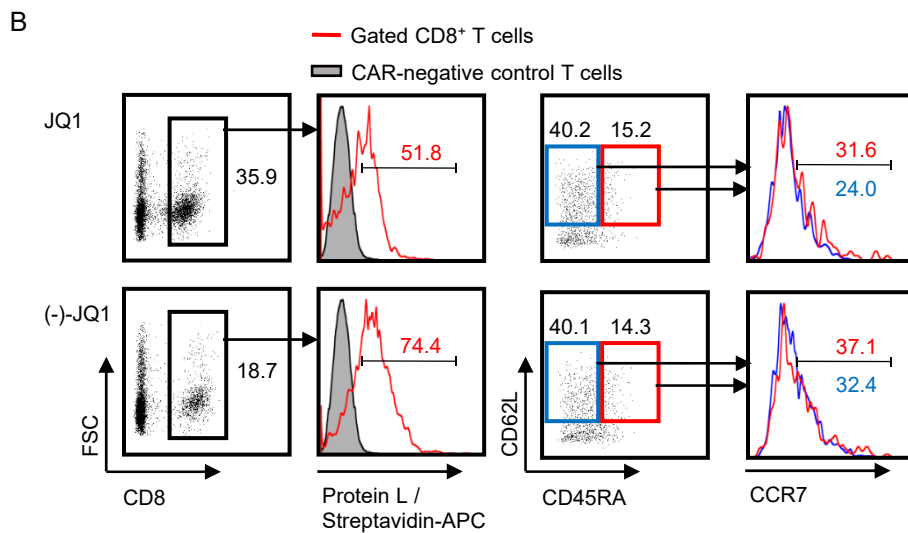
Supplemental Figure 11

A

B

Supplemental Figure 11. Treatment of CD19+ acute lymphoblastic cell line NALM-6 with anti-CD19 CAR-transduced T cells. (A) NSG mice were intravenously injected with NALM6-GL and, 14 days later, treated with CAR-transduced T cells treated with JQ1 or (-)-JQ1. *In vivo* bioluminescent imaging of luciferase activity at the indicated time points following T cell infusion is shown. (B) Phenotypic analysis for persistent CD8+ CAR-T cells in the peripheral blood. Representative FACS plots at day 7 following T cell infusion are shown.

A

JQ1-CAR-T cell transplanted mice

(-)-JQ1-CAR-T cell transplanted mice

Spleen   Bone marrow   Spleen   Bone marrow

61.8   66.0   38.4   55.8

In vitro cultured
NALM6-GL

GFP

CD19

— GFP⁺ cells
— K562

B

JQ1   0.57   60.5   5.76

Residual CD8⁺ T cells
Control T cells

(-)-JQ1   3.24   75.6   0.65

FSC   CD45   CD4   CD8   Protein L /
Streptavidin-PE

Supplemental Figure 12. Autopsy analysis of mice transplanted with JQ1- or (-)-JQ1-CAR-T cells. (A) Representative FACS plots evaluating the persistence of NALM6-GL and CD19 expression in the spleen and bone marrow. (B) Representative FACS plots showing the persistence of CAR-T cells in the spleen.

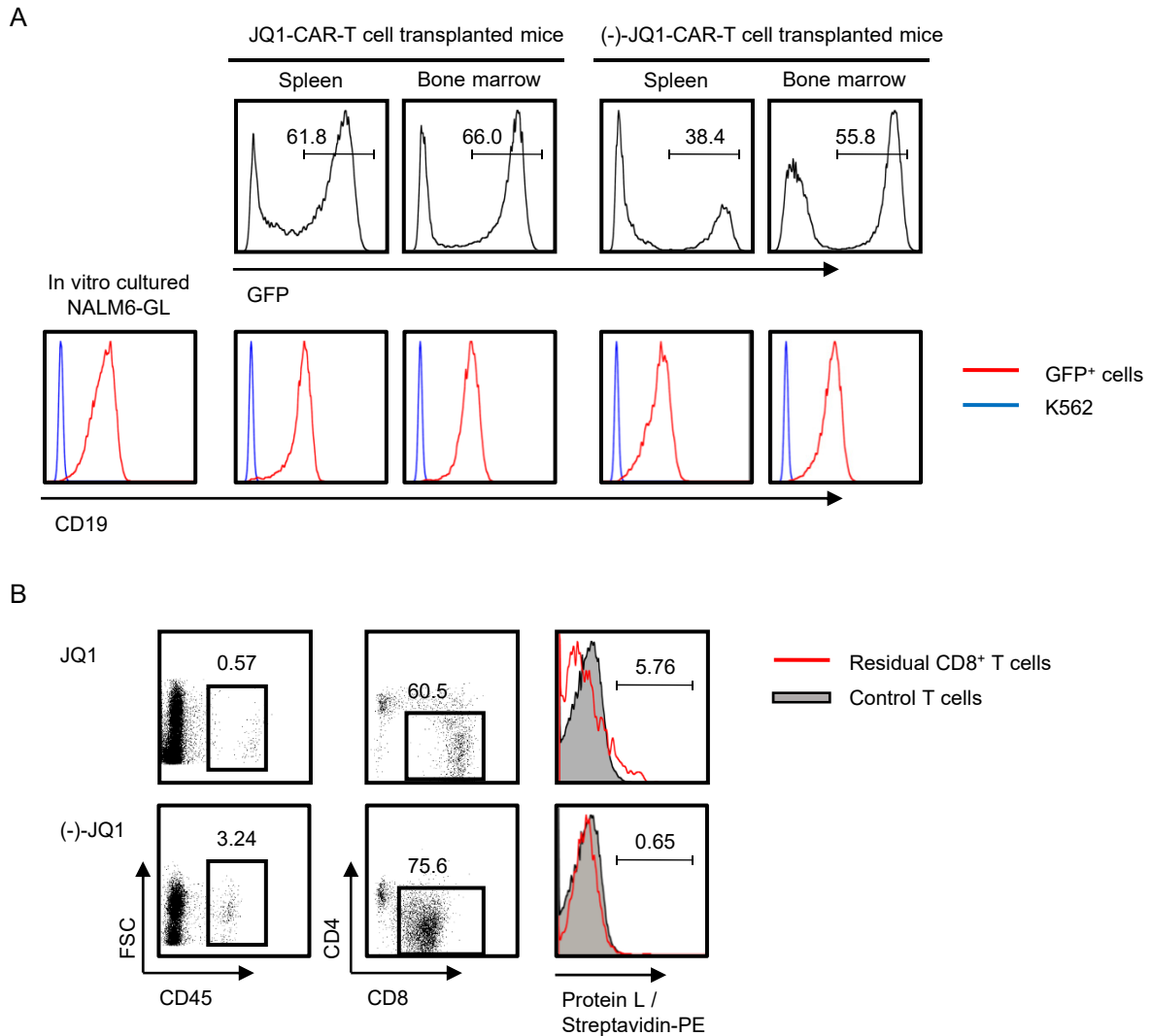**Supplemental Figure 13. Cytokine secretion by A2/MART1-T cells following restimulation with aAPC/A2.** JQ1- or (-)-JQ1-treated A2/MART1-T cells were stimulated with aAPC/A2 loaded with MART1$_{27\text{-}35}$ peptide in the absence of drugs. Five days later, the T cells were restimulated with aAPC/A2 with MART1$_{27\text{-}35}$, and cytokine secretion was evaluated by intracellular flow cytometry. Frequencies of each type of cytokine-producing cell and cells secreting all three cytokines are shown (n=4; paired t test).
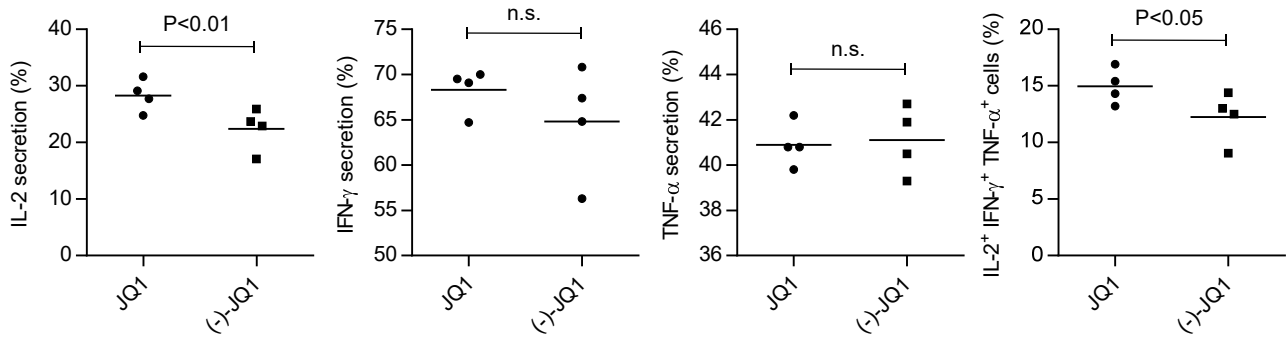
Supplemental Figure 14
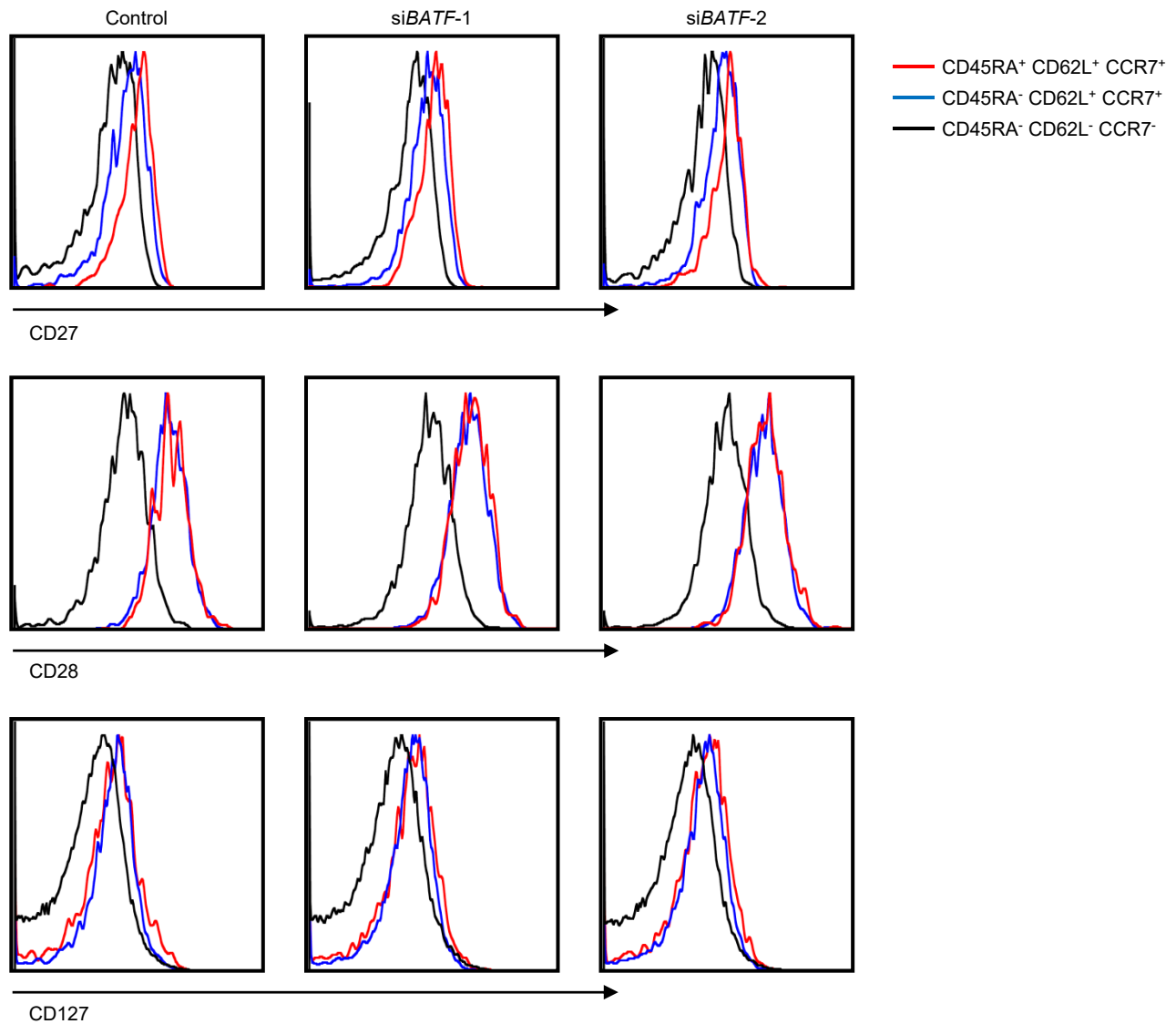
Supplemental Figure 14. Surface marker phenotypes of CD8$^+$ T cells with BATF knockdown. Surface expression of CD27, CD28, and CD127 in the CD8$^+$ ΔNGFR$^+$ T cells transduced with control or si*BATF* 14 days following initial stimulation with aAPC/mOKT3. Representative plots of the samples in Figure 7C are shown.

Supplemental Figure 15
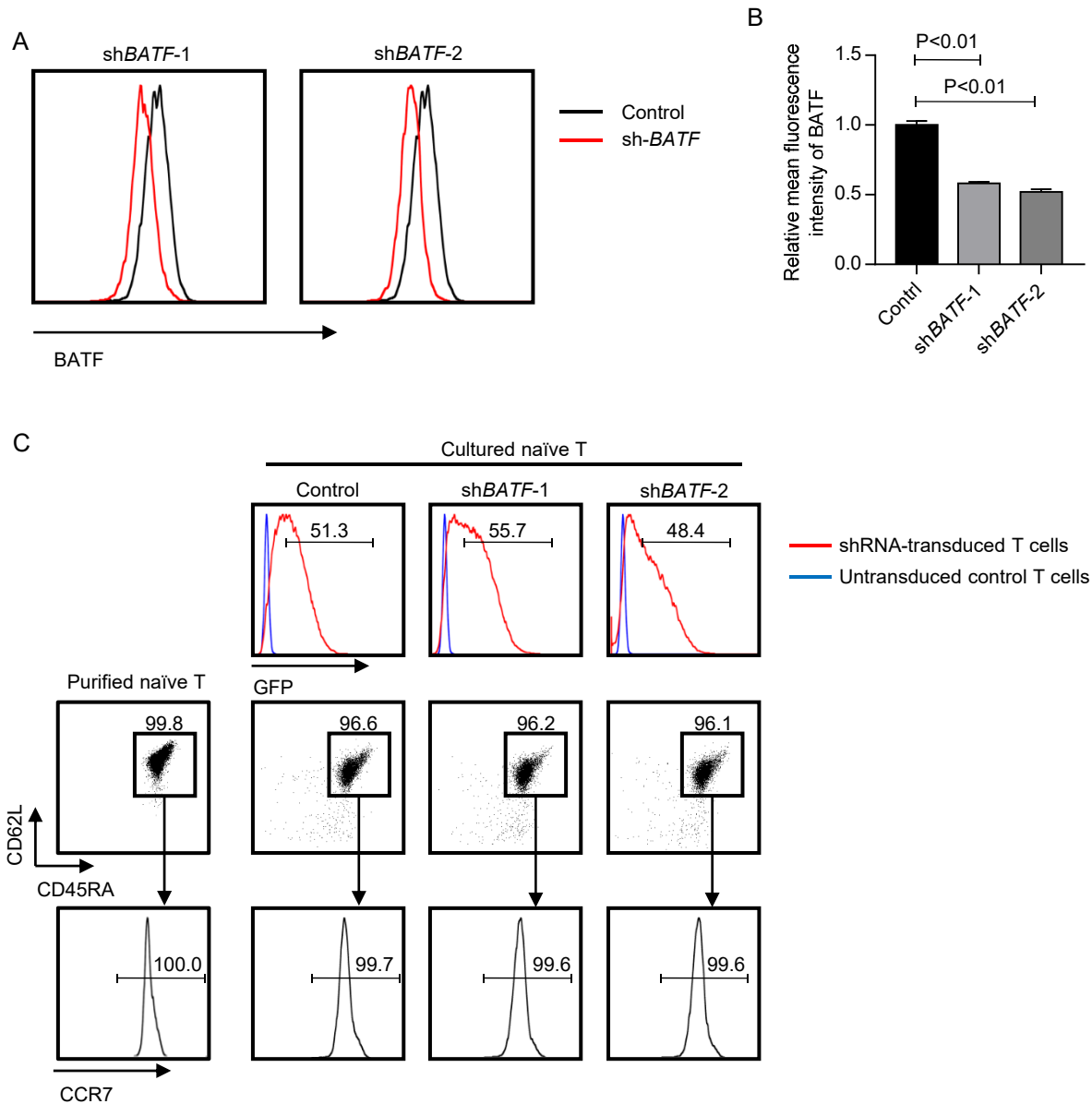
Supplemental Figure 15. BATF knockdown by lentiviral shRNA. (A, B) CD3$^+$ T cells were transduced with lentiviral shRNAs against BATF and stimulated with aAPC/mOKT3. Protein levels of BATF in the CD8$^+$ ZsGreen$^+$ T cell population were analyzed by intracellular flow cytometry three days following stimulation. Representative FACS plots (A) and average relative mean fluorescence intensity normalized to the control (B) (n=4; one-way ANOVA). Error bars indicate the S.D. (C) Naïve T cells were purified by magnetic selection, pre-treated with IL-7, and transduced with lentiviral shRNA targeting BATF at day 5-8. Representative FACS plots of CD45RA, CD62L and CCR7 expression in the purified naïve T cells and after shRNA transduction are shown.

Supplemental Figure 16
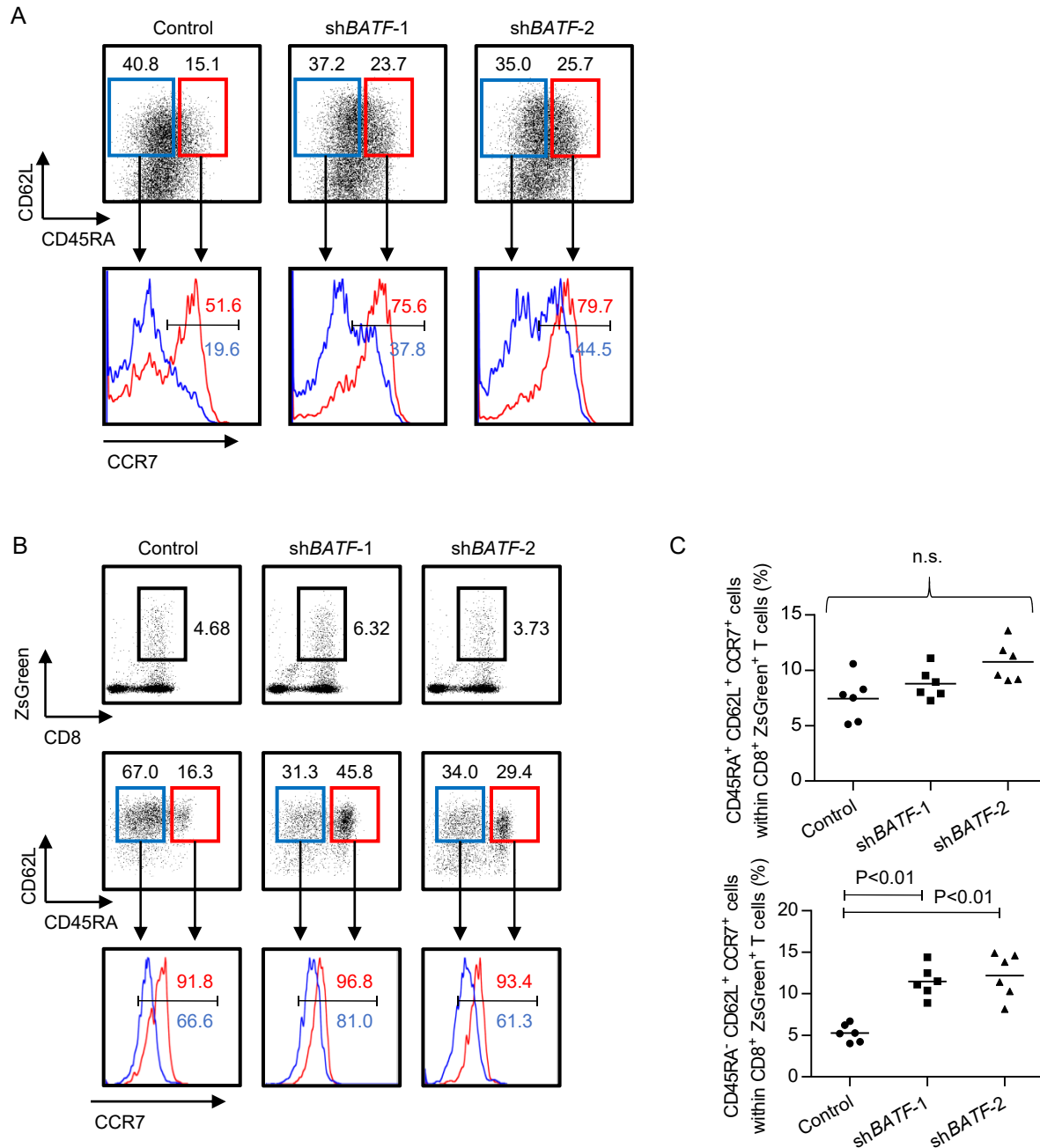
Supplemental Figure 16. Memory T cell formation from naïve T cells transduced with lentiviral shRNA against BATF. (A) Naïve T cells were transduced with shRNA against BATF following pretreatment with IL-7. They were subsequently stimulated with aAPC/mOKT3, and the expression profiles of CD45RA, CD62L and CCR7 within the CD8$^+$ ZsGreen$^+$ T cell population were analyzed 10 days following stimulation. Representative FACS plots of the five experiments are shown. (B) Naïve T cells transduced with shRNA against BATF were transplanted into irradiated NSG mice. Mice were sacrificed 11 days following T cell infusion, and the CD8$^+$ ZsGreen$^+$ cells engrafted in the spleen were analyzed. Representative FACS plots analyzing expression of CD45RA, CD62L and CCR7 within the CD45$^+$ CD8$^+$ ZsGreen$^+$ population are shown. (C) Naïve T cells with shRNA against BATF were transplanted into irradiated NSG mice, as shown in Figure 7H. Mice were sacrificed 16 days following T cell infusion, and the frequency of CD45RA$^{+/-}$ CD62L$^+$ CCR7$^+$ cells within the ZsGreen$^+$ CD8$^+$ T cell population in the spleen was analyzed (n=6, one-way ANOVA).

Supplemental Figure 17. Knockdown effects of genes suppressed by JQ1 on memory T cell differentiation. (A) Expression of the candidate genes targeted by JQ1 was assessed by quantitative real-time PCR. Relative expression levels of the indicated genes in JQ1-treated T cells relative to (-)-JQ1-treated cells (normalized to UBC) three days after stimulation with aAPC/mOKT3 are shown (n=4, one-sample test compared to one). Error bars indicate the S.D. ND, not detected within 45 cycles of qPCR. * P<0.05, ** P<0.01. (B) CD3$^+$ T cells were retrovirally transduced with the control, si*FOSL2*, si*ID2*, or si*PRDM1* and ΔNGFR. Expression of each target gene compared with the control was assessed by quantitative PCR (n=4, one sample t test compared to one). Error bars indicate the S.D. * P<0.05, ** P<0.01. (C) CD3$^+$ T cells were stimulated with aAPC/mOKT3 and transduced with control, si*FOSL2*, si*ID2*, or si*PRDM1*, and ΔNGFR. The frequency of CD45RA$^{+/-}$ CD62L$^+$ CCR7$^+$ cells within the ΔNGFR$^+$ CD8$^+$ T cell population 14 days after initial stimulation is shown (n=5, paired ANOVA).
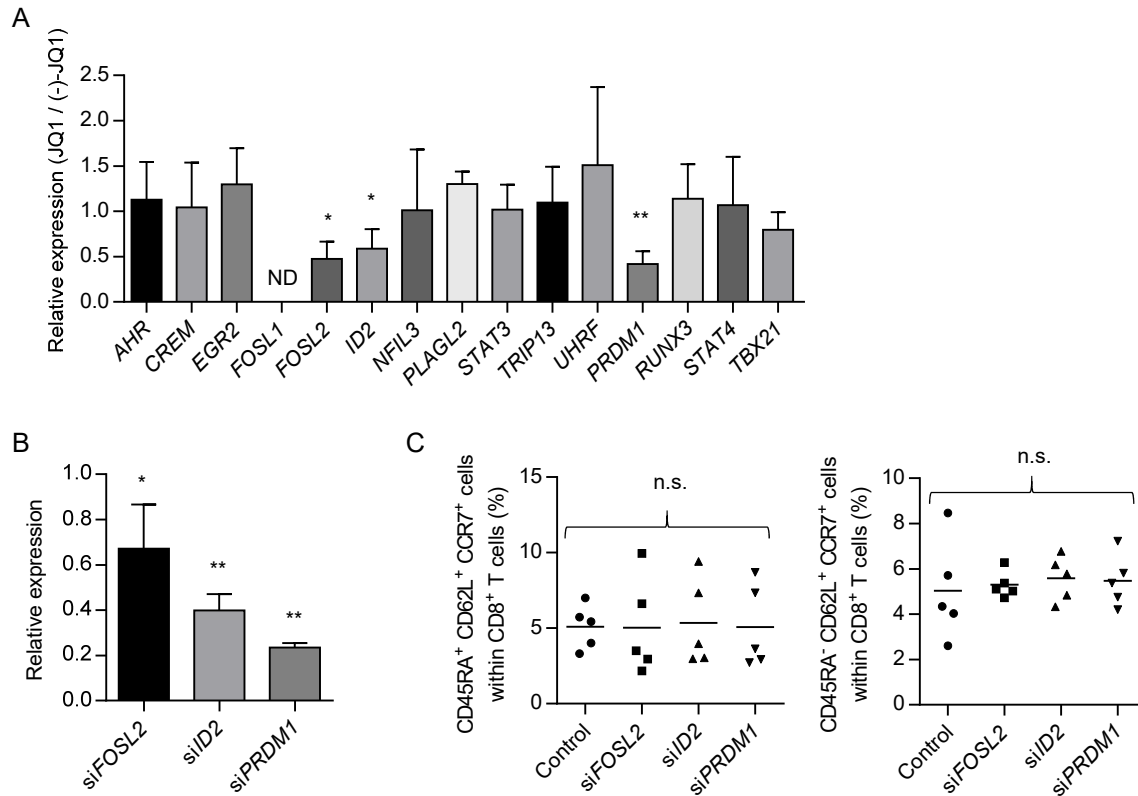
A

pSTAT5   p-p38 MAPK   pERK   pAKT   pS6K

—— JQ1
—— (-)-JQ1
—— Day 0 CD8+ T cells

B

C

pS6K

—— Control
—— sh*BATF*-1
—— sh*BATF*-2

D
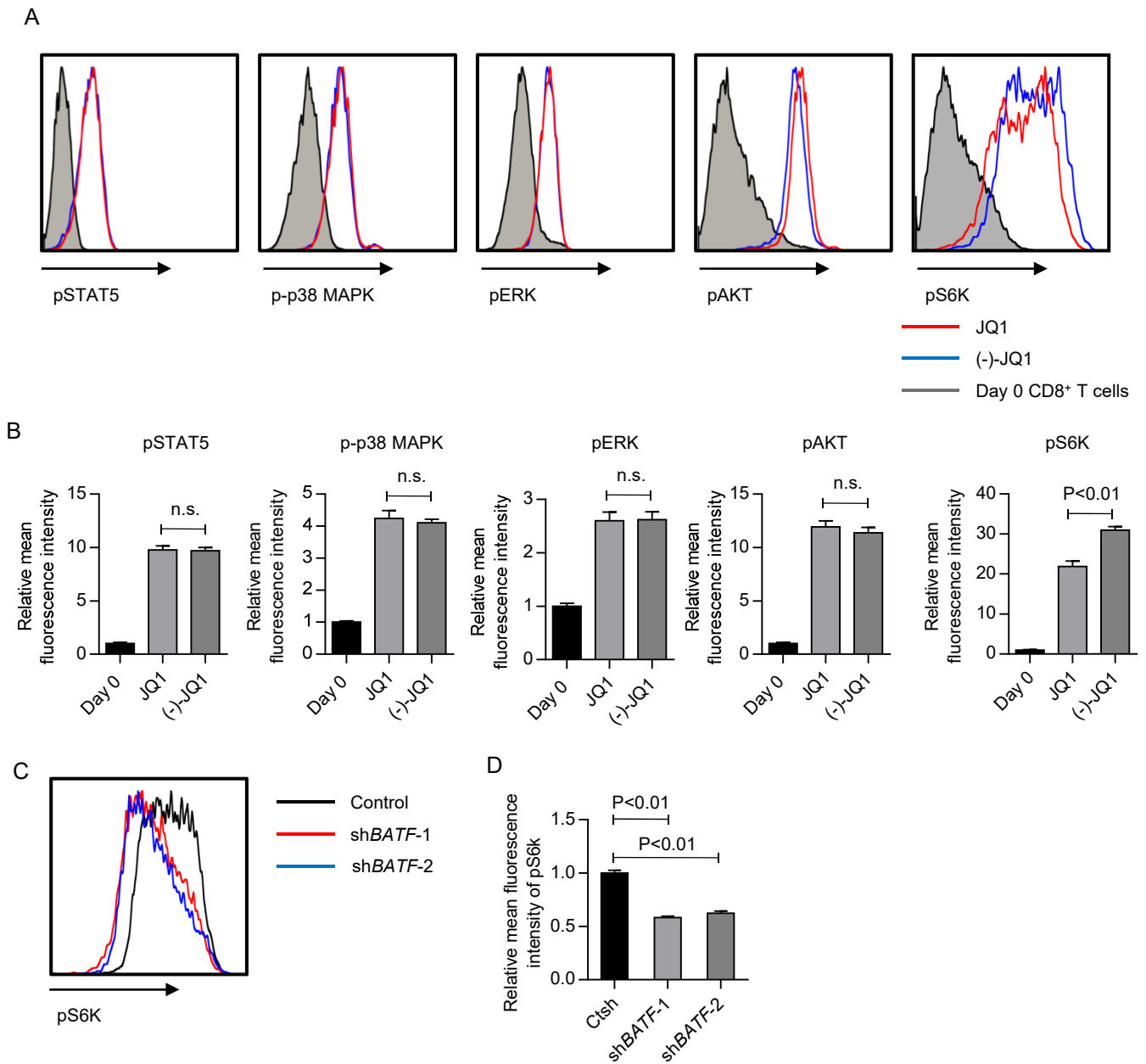
Supplemental Figure 18. Phosphorylation of ribosomal protein S6 kinase (S6K) is decreased in JQ1-treated T cells. (A, B) CD3+ T cells were stimulated with aAPC/mOKT3 at an E:T ratio of 3:1 and treated with JQ1 or (-)-JQ1 in the presence of IL-2 and IL-15. Phosphorylation of the indicated proteins in CD8+ T cell population was analyzed 5 days after stimulation. Representative FACS plots (A) and relative mean fluorescence intensity normalized to freshly isolated CD8+ T cells (B) (n=4; unpaired t test). (C, D) CD3+ T cells were stimulated with aAPC/mOKT3 and transduced with lentiviral shRNA against BATF. The shRNA-transduced T cells were rested in cytokine-free media and then restimulated with aAPC/mOKT3. Phosphorylation of S6K in the ZsGreen+ CD8+ T cell population was quantified by intracellular flow cytometry. Representative FACS plots (C) and relative mean fluorescence intensity normalized to the control plasmid-transduced cells (D) (n=4; one-way ANOVA).

Supplemental Figure 19. Phenotypic analysis of CAR-T cells after adoptive transfer. C646- or DMSO-treated CAR-T cells were infused into NSG mice transplanted with NALM6-GL. The frequency of CD45RA$^{+/-}$ CD62L$^+$ CCR7$^+$ T cells within the CD8$^+$ CAR$^+$ T cell population was analyzed (n=10, unpaired t test).
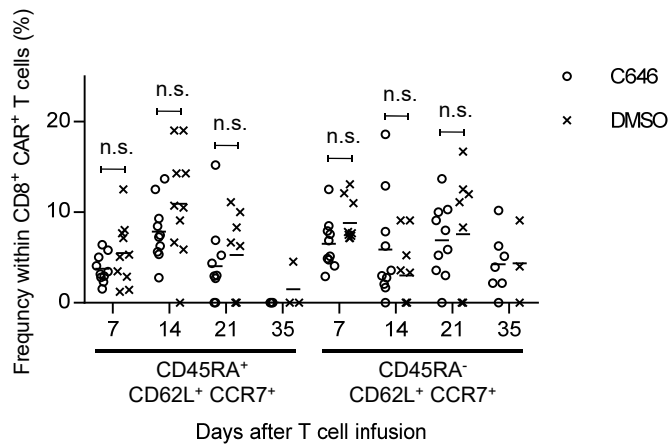
Supplemental Table 1. Epigenetic chemical probes with defined targets.

Probe	Target	Tested dose (μM)	References
Histone-modifying enzymes			
UNC0638	G9a/GLP	0.1	1
UNC0642	G9a/GLP	0.1	2
A-366	G9a/GLP	0.5	3
SGC0946	DOT1L	0.5	4
UNC1999	EZH2	0.2	5
GSK343	EZH2	0.5	6
GSK-J4	JMJD3/UTX	1	7
OICR-9429	WDR5	1	8
PFI-2	SETD7	1	9
GSK-LSD1	LSD1	1	10
UNC1215	L3MBTL3	1	11
SGC-CBP30	CREBBP/EP300	0.2	12
I-CBP112	CREBBP/EP300	1	13
C646	EP300	10	14

Probe	Target	Tested dose (μM)	References
Histone readers			
JQ1	BET Bromodomain	0.15	15
PFI-1	BET Bromodomain	1	16
Bromosporine	pan-Bromodomain	1	
GSK2801	BAZ2A/B	1	17
BAZ2-ICR	BAZ2B/A	1	18
OF-1	BRPF1-3	1	
Ni-57	BRPF1-3	0.5	
PFI-4	BRPF1B	0.25	
PFI-3	SMARCA4	1	19
CI-994	HDAC	1	
LAQ824	HDAC	0.01	20
VPA	HDAC	400	
Other targets			
Olaparib	PARP	1	
IOX2	HIF1a	50	21
GSK484	PAD-4	0.5	22
LLY-507	SMYD2	1	23
Decitabine	DNMT	0.05	

Supplemental Table 2. Detailed information of the mice transplanted with CAR-T cells.

| | Probe | Overall survival | NALM6-GL at autopsy (%) | | CAR-T cell at autopsy (%) | | | | | | | | Signs of GVHD |
| | | | Bone marrow | Spleen | T cells in the bone marrow | | | | T cells in the spleen | | | | |
					CD4$^+$	CD8$^+$	CAR$^+$ in CD4$^+$ T cells	CAR$^+$ in CD8$^+$ T cells	CD4$^+$	CD8$^+$	CAR$^+$ in CD4$^+$ T cells	CAR$^+$ in CD8$^+$ T cells	
1	JQ1	85	35.6	25.2	2.02	0.46	0.53	1.56	7.25	0.93	0.41	2	fur loss and red skin
2		64	67.8	42.8	0.56	0.08	3.60	6.56	0.38	0.08	1.23	6.92	none
3		65	66	61.8	0.06	0.06	2.60	7.55	0.11	0.35	2.34	5.76	none
4		59	24.6	14.1	1.05	0.06	3.07	8.7	2.35	0.03	0.00	2.13	none
5		91 (alive)	NA										fur loss and red skin
6		91 (alive)	NA										none
7		45	66.1	21.6	0.40	0.02	1.36	4	0.35	0.02	0.76	0	none
8		91 (alive)	NA										none
9		33	73.2	35.2	0.05	0.02	6.12	0.00	0.06	0.05	2.72	5.17	none
10		46	45.1	33	0.01	0.06	0.00	1.79	0.00	0.01	0.00	0	none
1	(-)-JQ1	40	82.3	22.4	0.02	0.05	0.00	0	0.53	1.78	0.89	0.484	none
2		41	84.2	48.5	0.06	0.23	2.33	6.44	0.30	2.45	0.86	0.649	none
3		37	83.4	48.6	0.04	0.23	4.00	2.76	0.10	1.00	0.00	0.813	none
4		54	55.8	38.4	0.00	0.00	NA	NA	0.00	0.02	NA	0	none
5		61	28.4	16.8	0.07	0.02	2.71	12.3	0.79	0.21	0.89	3.39	none
6		46	82.6	45.3	0.21	0.27	1.32	2.11	0.28	1.54	0.63	0.794	none
7		36	72.9	22.2	0.02	0.00	5.88	NA	0.13	0.01	7.32	0	none
8		33	68.3	21.5	0.01	0.02	0.00	8.7	0.13	0.12	2.20	6.71	none
9		40	60.2	21.1	0.03	0.04	0.00	0	0.59	0.49	1.26	2.76	none
10		34	84.5	37.7	0.07	0.19	2.94	2.25	0.13	1.08	0.00	1.21	none

References

1. Vedadi M, Barsyte-Lovejoy D, Liu F, Rival-Gervier S, Allali-Hassani A, Labrie V, Wigle TJ, Dimaggio PA, Wasney GA, Siarheyeva A, et al. A chemical probe selectively inhibits G9a and GLP methyltransferase activity in cells. *Nat Chem Biol.* 2011;7(8):566-74.

2. Liu F, Barsyte-Lovejoy D, Li F, Xiong Y, Korboukh V, Huang XP, Allali-Hassani A, Janzen WP, Roth BL, Frye SV, et al. Discovery of an in vivo chemical probe of the lysine methyltransferases G9a and GLP. *J Med Chem.* 2013;56(21):8931-42.

3. Sweis RF, Pliushchev M, Brown PJ, Guo J, Li F, Maag D, Petros AM, Soni NB, Tse C, Vedadi M, et al. Discovery and development of potent and selective inhibitors of histone methyltransferase g9a. *ACS Med Chem Lett.* 2014;5(2):205-9.

4. Yu W, Chory EJ, Wernimont AK, Tempel W, Scopton A, Federation A, Marineau JJ, Qi J, Barsyte-Lovejoy D, Yi J, et al. Catalytic site remodelling of the DOT1L methyltransferase by selective inhibitors. *Nat Commun.* 2012;3(1288.

5. Konze KD, Ma A, Li F, Barsyte-Lovejoy D, Parton T, Macnevin CJ, Liu F, Gao C, Huang XP, Kuznetsova E, et al. An orally bioavailable chemical probe of the Lysine Methyltransferases EZH2 and EZH1. *ACS Chem Biol.* 2013;8(6):1324-34.

6. Verma SK, Tian X, LaFrance LV, Duquenne C, Suarez DP, Newlander KA, Romeril SP, Burgess JL, Grant SW, Brackley JA, et al. Identification of Potent, Selective, Cell-Active Inhibitors of the Histone Lysine Methyltransferase EZH2. *ACS Med Chem Lett.* 2012;3(12):1091-6.

7. Kruidenier L, Chung CW, Cheng Z, Liddle J, Che K, Joberty G, Bantscheff M, Bountra C, Bridges A, Diallo H, et al. A selective jumonji H3K27 demethylase inhibitor modulates the proinflammatory macrophage response. *Nature.* 2012;488(7411):404-8.

8. Grebien F, Vedadi M, Getlik M, Giambruno R, Grover A, Avellino R, Skucha A, Vittori S, Kuznetsova E, Smil D, et al. Pharmacological targeting of the Wdr5-MLL interaction in C/EBPalpha N-terminal leukemia. *Nat Chem Biol.* 2015;11(8):571-8.

9. Barsyte-Lovejoy D, Li F, Oudhoff MJ, Tatlock JH, Dong A, Zeng H, Wu H, Freeman SA, Schapira M, Senisterra GA, et al. (R)-PFI-2 is a potent and selective inhibitor of SETD7 methyltransferase activity in cells. *Proc Natl Acad Sci U S A.* 2014;111(35):12853-8.

10. Mohammad HP, Smitheman KN, Kamat CD, Soong D, Federowicz KE, Van Aller GS, Schneck JL, Carson JD, Liu Y, Butticello M, et al. A DNA Hypomethylation Signature Predicts Antitumor Activity of LSD1 Inhibitors in SCLC. *Cancer Cell.* 2015;28(1):57-69.

11. James LI, Barsyte-Lovejoy D, Zhong N, Krichevsky L, Korboukh VK, Herold JM, MacNevin CJ, Norris JL, Sagum CA, Tempel W, et al. Discovery of a chemical probe for the L3MBTL3 methyllysine reader domain. *Nat Chem Biol.* 2013;9(3):184-91.

12. Hay DA, Fedorov O, Martin S, Singleton DC, Tallant C, Wells C, Picaud S, Philpott M, Monteiro OP, Rogers CM, et al. Discovery and optimization of small-molecule ligands for the CBP/p300 bromodomains. *J Am Chem Soc.* 2014;136(26):9308-19.

13. Picaud S, Fedorov O, Thanasopoulou A, Leonards K, Jones K, Meier J, Olzscha H, Monteiro O, Martin S, Philpott M, et al. Generation of a Selective Small Molecule Inhibitor of the CBP/p300 Bromodomain for Leukemia Therapy. *Cancer Res.* 2015;75(23):5106-19.

14. Bowers EM, Yan G, Mukherjee C, Orry A, Wang L, Holbert MA, Crump NT, Hazzalin CA, Liszczak G, Yuan H, et al. Virtual ligand screening of the p300/CBP histone acetyltransferase: identification of a selective small molecule inhibitor. *Chem Biol.* 2010;17(5):471-82.

15. Filippakopoulos P, Qi J, Picaud S, Shen Y, Smith WB, Fedorov O, Morse EM, Keates T, Hickman TT, Felletar I, et al. Selective inhibition of BET bromodomains. *Nature.* 2010;468(7327):1067-73.

16. Picaud S, Da Costa D, Thanasopoulou A, Filippakopoulos P, Fish PV, Philpott M, Fedorov O, Brennan P, Bunnage ME, Owen DR, et al. PFI-1, a highly selective protein interaction inhibitor, targeting BET Bromodomains. *Cancer Res.* 2013;73(11):3336-46.

17. Chen P, Chaikuad A, Bamborough P, Bantscheff M, Bountra C, Chung CW, Fedorov O, Grandi P, Jung D, Lesniak R, et al. Discovery and Characterization of GSK2801, a Selective Chemical Probe for the Bromodomains BAZ2A and BAZ2B. *J Med Chem.* 2015.

18.   Drouin L, McGrath S, Vidler LR, Chaikuad A, Monteiro O, Tallant C, Philpott M, Rogers C, Fedorov O, Liu M, et al. Structure enabled design of BAZ2-ICR, a chemical probe targeting the bromodomains of BAZ2A and BAZ2B. *J Med Chem.* 2015;58(5):2553-9.

19.   Vangamudi B, Paul TA, Shah PK, Kost-Alimova M, Nottebaum L, Shi X, Zhan Y, Leo E, Mahadeshwar HS, Protopopov A, et al. The SMARCA2/4 ATPase Domain Surpasses the Bromodomain as a Drug Target in SWI/SNF-Mutant Cancers: Insights from cDNA Rescue and PFI-3 Inhibitor Studies. *Cancer Res.* 2015;75(18):3865-78.

20.   Catley L, Weisberg E, Tai YT, Atadja P, Remiszewski S, Hideshima T, Mitsiades N, Shringarpure R, LeBlanc R, Chauhan D, et al. NVP-LAQ824 is a potent novel histone deacetylase inhibitor with significant activity against multiple myeloma. *Blood.* 2003;102(7):2615-22.

21.   Chowdhury R, Candela-Lena JI, Chan MC, Greenald DJ, Yeoh KK, Tian YM, McDonough MA, Tumber A, Rose NR, Conejo-Garcia A, et al. Selective small molecule probes for the hypoxia inducible factor (HIF) prolyl hydroxylases. *ACS Chem Biol.* 2013;8(7):1488-96.

22.   Lewis HD, Liddle J, Coote JE, Atkinson SJ, Barker MD, Bax BD, Bicker KL, Bingham RP, Campbell M, Chen YH, et al. Inhibition of PAD4 activity is sufficient to disrupt mouse and human NET formation. *Nat Chem Biol.* 2015;11(3):189-91.

23.   Nguyen H, Allali-Hassani A, Antonysamy S, Chang S, Chen LH, Curtis C, Emtage S, Fan L, Gheyi T, Li F, et al. LLY-507, a Cell-active, Potent, and Selective Inhibitor of Protein-lysine Methyltransferase SMYD2. *J Biol Chem.* 2015;290(22):13641-53.